

# On Finding Bi-objective Pareto-optimal Fraud Prevention Rule Sets for Fintech Applications

Chengyao Wen  
Ant Group  
Chengdu, China  
wenchengyao.wcy@antgroup.com

Yin Lou  
Ant Group  
Sunnyvale, CA, USA  
yin.lou@antgroup.com

## ABSTRACT

Rules are widely used in Fintech institutions to make fraud prevention decisions, since rules are highly interpretable thanks to their intuitive if-then structure. In practice, a two-stage framework of fraud prevention decision rule set mining is usually employed in large Fintech institutions. This paper is concerned with finding high-quality rule subsets in a bi-objective space (such as precision and recall) from an initial pool of rules. To this end, we adopt the concept of Pareto optimality and aim to find a set of non-dominated rule subsets, which constitutes a Pareto front. We propose a heuristic-based framework called PORS and we identify that the core of PORS is the problem of solution selection on the front (SSF). We provide a systematic categorization of the SSF problem and a thorough empirical evaluation of various SSF methods on both public and proprietary datasets. We also introduce a novel variant of sequential covering algorithm called SpectralRules to encourage the diversity of the initial rule set and we empirically find that SpectralRules further improves the quality of the found Pareto front. On two real application scenarios within Alipay, we demonstrate the advantages of our proposed methodology compared to existing work.

## CCS CONCEPTS

• **Computing methodologies** → **Rule learning.**

## KEYWORDS

multi-objective optimization, Pareto front, rule subset selection

## ACM Reference Format:

Chengyao Wen and Yin Lou. 2018. On Finding Bi-objective Pareto-optimal Fraud Prevention Rule Sets for Fintech Applications. In *Proceedings of Make sure to enter the correct conference title from your rights confirmation email (Conference acronym 'XX)*. ACM, New York, NY, USA, 10 pages. <https://doi.org/XXXXXXXX.XXXXXXX>

## 1 INTRODUCTION

Fraud prevention is an important task in Fintech applications. Fraudulent activities usually include identity theft, money laundering, fraudulent payment transactions, etc. Whenever a fraud is committed,

the loss is not only incurred by the victim who is exploited, but the reputation of the financial institution involved also takes a hit.

In many Fintech fraud prevention applications, interpretability is usually a must-have requirement in addition to predictive accuracy. Therefore, rule-based models are widely used for such applications to make fraud prevention decisions, since rules can offer intuitive representation of knowledge, thanks to their simple if-then structure. In practice, decision rule sets (also known as disjunctive normal form) are often favored over decision rule list due to their flatter representation [13]; rule set models make positive prediction for a transaction whenever any rule in the set is satisfied. During any stage in a transaction, whenever an alert is made from the rule set (i.e., at least one rule predicts positive on this transaction), the transaction is interrupted and the user may be asked to submit additional information to verify the legitimacy for this transaction.

In practice, a two-stage framework of rule set mining is commonly employed in Fintech institutions (e.g., Alipay<sup>1</sup>) [16]. In Stage 1, a (potentially large) pool of rules is generated. Stage 2 is to produce a refined rule subset according to some criteria. Note that in this paper we use rule set to refer to rules generated by Stage 1 and rule subset to refer to a refined subset of the initial pool of rules *after* Stage 1.

There are many methods for generating the initial pool of rules for Stage 1. Tree based approaches, such as decision tree [6, 20] or random forests [5], extract rules for each path in the tree. Another class of approaches, on the other hand, focuses on direct rule induction to form rule sets. Popular methods in this category include sequential covering [17] (e.g., CN2 [9] and RIPPER [10]) and association rule mining [2].

For Stage 2, it is widely accepted that rule subsets are evaluated by their precision and recall [16]. Precision in our context is negatively correlated with the frequency that a user experiences an interruption for a transaction, and recall relates to the amount of fraudulent activities that can be prevented for a financial institution. Note that these two objectives are naturally conflicting with each other, and in practice one either seeks to maximize recall constrained on some precision threshold [16], or combines the two metrics into a single generalized  $F$  score that can balance the effects of the two objectives.  $F$  score uses a parameter  $\beta$  to control the contribution of the two inputs;  $\beta$  is chosen such that recall is considered  $\beta$  times as important as precision [23]. A large  $\beta$  weighs recall higher than precision and a small  $\beta$  is more biased towards precision. The commonly used  $F_1$  score is just a special case when  $\beta = 1$ . For fraud prevention problems in Fintech applications, typically a small  $\beta$  (e.g., 0.1) is used to give more weights on precision, since usually the fraudulent ratio is low.

Permission to make digital or hard copies of all or part of this work for personal or classroom use is granted without fee provided that copies are not made or distributed for profit or commercial advantage and that copies bear this notice and the full citation on the first page. Copyrights for components of this work owned by others than ACM must be honored. Abstracting with credit is permitted. To copy otherwise, or republish, to post on servers or to redistribute to lists, requires prior specific permission and/or a fee. Request permissions from [permissions@acm.org](mailto:permissions@acm.org).

*Conference acronym 'XX, June 03–05, 2018, Woodstock, NY*

© 2018 Association for Computing Machinery.  
ACM ISBN 978-1-4503-XXXX-X/18/06...\$15.00  
<https://doi.org/XXXXXXXX.XXXXXXX>

<sup>1</sup><https://www.alipay.com/>

In practice, however, one rarely knows beforehand the best constraint threshold or  $\beta$  for a particular problem, and rule mining is an *explorative* and *iterative* process. For example, one might experiment multiple precision thresholds and choose the selected rule subset according to subjective preferences or domain knowledge [16]. In such cases, multiple trials of the rule subset selection algorithm are necessary, which is quite time consuming. Therefore, in this work we aim to find a set of Pareto-optimal solutions *all at once* in a bi-objective space of precision and recall, i.e., rule subsets in which one objective cannot be improved without worsening the other one. A solution (rule subset) Pareto-dominates another one if both its precision and recall are no worse and at least one is strictly better. The image of this non-dominated solution set in the objective space is the so-called Pareto front.

Finding Pareto-optimal rule subsets can be viewed as an intermediate step between Stage 1 and Stage 2. It takes the initial pool of rules from Stage 1 and generates a set of non-dominated rule subsets. As a result, one can easily experiment different precision thresholds or  $\beta$  on the (already generated) Pareto-optimal solution set and choose one as the final output for Stage 2. For example, if the goal is to maximize recall constrained on precision  $\geq 0.9$ , one can simply filter all Pareto-optimal solutions whose precision is lower than 0.9 and choose the one with the highest recall, and therefore avoids the need to experiment multiple precision thresholds.

The hypervolume indicator (HV) is one of the most widely used evaluation metric for the quality of a Pareto front [15]. It measures the “size of the dominated space” [26], and our goal for this paper is to find Pareto front of large HV. In this work, we mainly focus on a bi-objective space of precision and recall, and measure the dominated space referenced by (0, 0) (See Figure 1 for a visual example). Each solution on a Pareto front forms a rule subset.

This problem can be solved by standard evolutionary multi-objective optimization (EMO) algorithms, since bi-objective optimization is just a special case [14, 22]. Popular EMO algorithms include NSGA-II [11], MOEA/D [25], etc. However, we empirically find EMO algorithms are less efficient for our problem.

In this work, we propose a heuristic-based framework called PORS of finding Pareto-optimal solutions for rule subset selection problem. PORS gradually “expands” the Pareto front by adding one rule to a solution (rule subset) on the front to see whether it expands the front (thereby improves HV), and it terminates when no expansion of the current front can move the needle. Due to the combinatorial nature of this problem, it is computationally prohibitive to enumerate all rule subsets on the current Pareto front, and therefore we only select a set of *representative* solutions on the current front as candidates for expansion to avoid exponential growth. We refer to this problem as solution selection on the front (SSF).

A closely related problem of SSF is the so-called subset selection of Pareto-optimal solutions, in which the goal is to reduce the number of solutions on a Pareto front to a user specified number while achieving some desired properties (e.g., a high HV approximation of the original Pareto front). Popular methods of Pareto subset selection include HV-SS [8], IGD/IGD+-SS [8], etc. Our motivation is different in that we are interested in finding a small set of promising solutions to expand on the current front so as to achieve a high HV when PORS terminates. We can, nevertheless, employ existing algorithms in PORS.

Sampling	Space	Method
Uniform	Objective	equi-spaced [18] equi-dist (this paper)
	Non-objective	equi-jaccard (this paper)
Non-uniform	Objective	hv-ss [8] igd-ss [8] igd+-ss [8] hvc-ss (this paper) k-medoids-pr [7]
	Non-objective	k-medoids-jaccard (this paper)

**Table 1: Categorization of SSF methods.**

Since finding a small set of most promising solutions to expand on the current front is at the core of our framework, as one of our contributions, we propose a systematic categorization of solutions to this problem, map existing methods into different categories, and conduct a thorough empirical evaluation of methods in each category for SSF problem to study their effects on the quality of final Pareto front. If we think of the front as a “curve” in some space, we can broadly classify methods into two categories; uniform or non-uniform sampling on the “curve.” The space could be the objective space (e.g., bi-objective space of precision and recall in this paper) which is usually a coordinate system, or non-objective space (and therefore potentially non-coordinate system) where only distance metric of two rule subsets is defined (e.g., Jaccard distance between two rule subsets). Table 1 summarizes existing methods and the methods proposed in this paper into each category.

Although there are benchmark studies on subset selection of Pareto-optimal solutions [21] in the context of EMO, there is little research of finding Pareto-optimal rule subsets; not only EMO-based methods but greedy heuristic-based approaches considered in this paper as well. We believe our work provides a valuable piece of research in this area. Our empirical study on both public datasets and proprietary datasets from Alipay reveals that the proposed *hvc-ss* is the best SSF method, which achieves highest HV on almost all cases. In addition, we also propose a novel variant of the sequential covering algorithm [17] called *SpectralRules* that encourages the diversity of rules for Stage 1; *SpectralRules* generates a set of rules with different levels of precision and recall. We empirically find that *SpectralRules* usually generates a much smaller rule set in Stage 1 with highly diversified rules, leading to better computational efficiency for Stage 2, and benefits Stage 2 accordingly with final rule subsets of higher quality.

In summary, we make the following contributions in this paper.

- We propose a heuristic-based framework called PORS for finding Pareto-optimal rule subsets in a bi-objective space. At the core of this framework is the SSF problem.
- We provide a systematic categorization of the SSF problem and a thorough empirical evaluation of various SSF methods on both public and proprietary datasets. We find that the proposed *hvc-ss* is the best method for our problem.
- We propose a novel variant of the sequential covering algorithm called *SpectralRules* to encourage the diversity of

the initial pool rules, and demonstrate on both public and proprietary datasets that SpectralRules further improves HV.

- We present two case studies of using PORS in this paper to produce fraud prevention rule subsets for applications inside Alipay, and demonstrate the advantages of our methodology compared to existing work.
- We release a repository of code that can fully reproduce our results on public datasets in this study to promote research efforts in this area [1].

The rest of this paper is organized as follows. Section 2 presents related work. We present preliminaries in Section 3. Our approach is discussed in Section 4. Experimental results are presented in Section 5 and we conclude the paper in Section 6.

## 2 RELATED WORK

### 2.1 Rule Set Mining

There are generally two classes of approaches to generating rule sets. Tree based approaches, such as decision tree [6, 20] or random forests [5], extract rules for each path in the tree or tree ensemble. The other class of approaches focuses on direct rule induction to form rule sets. Popular methods of this category include sequential covering [17] (e.g., CN2 [9] and RIPPER [10]) and association rule mining [2]. Recently there is another line of research that focuses on the diversity of rule sets [13, 24]. In practice, a two-stage framework of rule set mining is used in Fintech institutions such as Alipay [16]. The aforementioned methods are usually employed to generate an initial rule set, followed by a rule subset selection procedure that produces a refined rule subset according to some criteria.

### 2.2 Evolutionary Multi-Objective Optimization

The evolutionary multi-objective optimization (EMO) algorithm is a popular choice for solving multi-objective optimization problems [14, 22]. EMO algorithms can be roughly classified into three categories; dominance-based approach, decomposition-based approach and indicator-based approach. Dominance based EMO algorithms commonly use Pareto dominance relationship and distance-based density estimation in the objective space for offspring generation and environmental selections. NSGA-II [11] and SPEA2 [27] are well-known and widely used dominance based EMO algorithms, which are believed to be very suitable for problems under 4 objectives [22]. Decomposition based approach decomposes a given multi-objective problem into single-objective sub-problems. MOEA/D is a representative decomposition based EMO algorithm [25]. Indicator based approaches employ a quantity indicator to evaluate or rank solutions. Popular approaches in this category include SMS-EMOA [4], HypE [3], etc. EMO algorithms are, however, typically inefficient on large problems. This paper employs a heuristic-based approach that achieves higher efficiency with better Pareto fronts.

### 2.3 Subset Selection of Pareto-optimal Solutions

Since the number of Pareto-optimal solutions can be very large for combinatorial optimization problems and infinity for continuous optimization problems, subset selection of Pareto-optimal solutions is usually an essential step. It is regarded as one of the most important topics in EMO domain, since it is involved in many phases

of EMO algorithms [7, 8]. It is also studied in the context of discrete approximation to the Pareto front for continuous optimization problems [18]. Some previous studies favor uniform sampling of the Pareto front [18] while others favor non-uniform sampling [7, 8, 12].

In this work, we further extend this categorization into 4 categories as listed in Table 1, which is not revealed in existing literature. Under this view, we present 4 new methods (one for each category) and perform a thorough empirical evaluation on both public and proprietary datasets in the context of fraud prevention rule set mining for Fintech applications.

## 3 PRELIMINARIES

Let  $\mathcal{D} = \{(\mathbf{x}_i, y_i)\}_{i=1}^N$  denote a dataset of size  $N$ , where  $\mathbf{x}_i = (x_{i1}, \dots, x_{ip})$  is a feature vector with  $p$  features for a transaction, and  $y_i \in \{0, 1\}$  indicates whether the corresponding transaction is reported fraud or not. We use  $\mathcal{P} = \{i|y_i = 1\}$  to denote the set of points with positive labels. We use  $\delta = |\mathcal{P}|/N$  to denote the positive ratio of  $\mathcal{D}$ .

A rule  $r$  has two parts; a conjunction of conditions and a prediction. A condition is of the form (feature, operator, value), e.g.,  $\text{age} > 50$ . A rule makes a certain prediction when all conditions are satisfied for a given  $\mathbf{x}_i$ . In this case, we say the rule covers  $\mathbf{x}_i$ . Since typically the positive ratio  $\delta$  for fraud in Fintech applications is very low, we only consider positive-class rules. Hence,  $r(\mathbf{x}_i) = 1$  iff  $r$  covers  $\mathbf{x}_i$ .

A rule set  $\mathcal{R}$  makes a positive prediction on  $\mathbf{x}_i$  if there exists a rule  $r \in \mathcal{R}$  such that  $r(\mathbf{x}_i) = 1$ . We use  $\mathcal{D}(\mathcal{R}) = \{i|R(\mathbf{x}_i) = 1\}$  to denote the set of data points covered by  $\mathcal{R}$ .

*Definition 3.1 (Precision).* We define the precision of a rule set  $\mathcal{R}$  as the percentage that  $\mathcal{R}$  correctly finds fraud,

$$\text{Prec}(\mathcal{R}) = \frac{|\mathcal{D}(\mathcal{R}) \cap \mathcal{P}|}{|\mathcal{D}(\mathcal{R})|}. \quad (1)$$

*Definition 3.2 (Recall).* We define the recall of a rule set  $\mathcal{R}$  as the ratio of the frauds covered by  $\mathcal{R}$  among all fraudulent transactions,

$$\text{Rec}(\mathcal{R}) = \frac{|\mathcal{D}(\mathcal{R}) \cap \mathcal{P}|}{|\mathcal{P}|}. \quad (2)$$

*Definition 3.3 ( $F_\beta$  score).* The general  $F_\beta$  score of precision and recall is defined as,

$$F_\beta = (1 + \beta^2) \frac{\text{precision} \times \text{recall}}{(\beta^2 \times \text{precision}) + \text{recall}}. \quad (3)$$

A large  $\beta$  weighs recall higher than precision, and a small  $\beta$  weighs precision higher than recall. For fraud prevention problems in Fintech applications, typically a small  $\beta$  (e.g., 0.1) is used to give more weights on precision, since usually the positive ratio (fraudulent ratio) is low.

Given a rule set  $\mathcal{R}$ , this paper is mostly concerned with finding high-quality rule subsets of  $\mathcal{R}$  in this bi-objective space of precision and recall.<sup>2</sup> To this end, we first introduce the concept of Pareto dominance.

*Definition 3.4 (Pareto dominance).* A rule subset  $\mathcal{R}_1$  is dominated by another rule subset  $\mathcal{R}_2$  if  $\text{Prec}(\mathcal{R}_1) \leq \text{Prec}(\mathcal{R}_2) \wedge \text{Rec}(\mathcal{R}_1) \leq \text{Rec}(\mathcal{R}_2)$  with at least one objective dimension (precision or recall) is strictly better. Under the context of Pareto dominance, we use rule subset and solution interchangeably.

<sup>2</sup>Nevertheless, our methodology can be easily extended to metrics other than precision and recall.

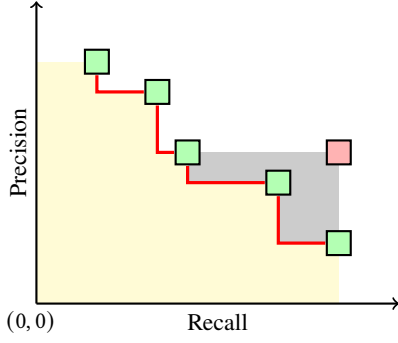


**Figure 1: Illustration of Pareto dominance.** A set of 5 non-dominated solutions (green square) constitutes the Pareto front (red line). Hypervolume of those 5 solutions is the size of the light yellow region. The hypervolume contribution of the solution (red square) to those 5 solutions is the size of the light grey region.

*Definition 3.5 (Pareto optimality).* A set of solutions (rule subsets) is called Pareto-optimal if no solution Pareto-dominates another.

*Definition 3.6 (Hypervolume Indicator).* Given a solution set  $S$  in a bi-objective space of precision and recall, the hypervolume indicator  $HV(S)$  is the measure of region dominated by  $S$ , referenced by  $(0, 0)$ .

Note that Pareto optimality only defines the situation where no solution can Pareto-dominate another *within* a solution set. One can, nevertheless, compare two sets of solutions that are both Pareto-optimal (via HV).

*Definition 3.7 (Hypervolume Contribution).* Given two solution sets  $S$  and  $\mathcal{T}$  in a bi-objective space of precision and recall, the hypervolume contribution of  $\mathcal{T}$  to  $S$  referenced by  $(0, 0)$  is,

$$HVC(\mathcal{T}, S) = HV(\mathcal{T} \cup S) - HV(S \setminus \mathcal{T}). \quad (4)$$

Figure 1 illustrates a set of 5 non-dominated solutions (green square) in a precision-recall space, which constitutes the Pareto front (red line). Hypervolume of those 5 solutions is the size of the light yellow region. The hypervolume contribution of a new solution (red square) to those 5 solutions is the size of the light grey region.

## 4 OUR APPROACH

In this section, we describe our methodology for finding Pareto-optimal rule subsets given an initial pool of rules  $\mathcal{R}$ . We first introduce a heuristic-based framework called PORS that gradually “expands” the Pareto front (Section 4.1). We identify solution selection on the front (SSF) as the core problem of this framework, and provide a systematic categorization of this problem. In Section 4.2, we map existing work into different category, and present new methods in each category. In addition, we introduce a novel variant of sequential covering algorithm called SpectralRules that encourages the diversity of the initial pool of rules  $\mathcal{R}$  for Stage 1 in Section 4.3.

### 4.1 The PORS Framework

PORS gradually “expands” the current Pareto front by adding one rule to a solution (rule subset) on the front to form a new set of solutions.

---

### Algorithm 1 The Pareto Optimal Rule Subset Selection Framework

---

```

1:  $\mathcal{F} \leftarrow \text{MAKEPF}(\{\{r\} | r \in \mathcal{R}\})$ 
2: converged  $\leftarrow$  false
3: while not converged do
4:   converged  $\leftarrow$  true
5:    $\mathcal{F}_0 \leftarrow \text{SSF}(\mathcal{F}, k)$ 
6:    $\mathcal{F}' \leftarrow \emptyset$ 
7:   for  $S \in \mathcal{F}_0$  do
8:     for  $r \in \mathcal{R}$  do
9:        $S' \leftarrow S \cup \{r\}$ 
10:       $\mathcal{F}' \leftarrow \mathcal{F}' \cup \{S'\}$ 
11:     $\mathcal{F}' \leftarrow \text{MAKEPF}(\mathcal{F}' \cup \mathcal{F})$ 
12:    converged  $\leftarrow \mathcal{F}' == \mathcal{F}$ 
13:   $\mathcal{F} \leftarrow \mathcal{F}'$ 
return  $\mathcal{F}$ 

```

---

Due to the combinatorial nature of this problem, it is computationally expensive to enumerate all rule subsets on the current Pareto front, and therefore we only select a set of *representative* solutions on the current front as candidates for expansion. We refer to this problem as solution selection on the front (SSF).

Algorithm 1 summarizes the proposed PORS framework for finding Pareto-optimal rule subsets given an initial pool of rules  $\mathcal{R}$ . The framework starts with singleton sets for each rule in  $\mathcal{R}$ , and then makes them a Pareto front via MAKEPF procedure by retaining only non-dominated solutions (Line 1). PORS applies some SSF method to sample  $k$  solutions on the current front in order to avoid exponential growth (Line 5). Those  $k$  solutions are then expanded by adding one rule from the initial pool of rules  $\mathcal{R}$  to form new solutions (Line 6-10). The expanded solutions are then put together with the solutions from last front to form a new Pareto front by retaining only non-dominated solutions (Line 11). The framework terminates when the current Pareto front does not change after expansion (Line 12), otherwise the current front is ready for the next iteration (Line 13).

It is obvious that the performance of PORS is largely affected by the efficacy of the SSF method, and therefore we discuss different candidate SSF methods in the next Section.

### 4.2 SSF Methods

We broadly classify SSF methods into two categories; uniform or non-uniform sampling on the “curve” of a Pareto front. Under each category, we identify two sub-categories depending on whether the “distance measure” is in the original objective space or not.

*4.2.1 Uniform Sampling.* We first discuss methods by uniform sampling in the objective space. We consider two methods in this paper as follows.

- **equi-spaced** [18]. [18] considers uniform sampling of the Pareto front in the objective space on continuous problems. In our problem, it is equivalent to uniform sampling of  $k$  solutions by walking along a Pareto front curve with roughly the same Manhattan distance for two consecutive samples.
- **equi-dist.** Following the same idea, we consider in this work uniform sampling of  $k$  solutions on a Pareto front with roughly the same Euclidean distance for two consecutive samples.

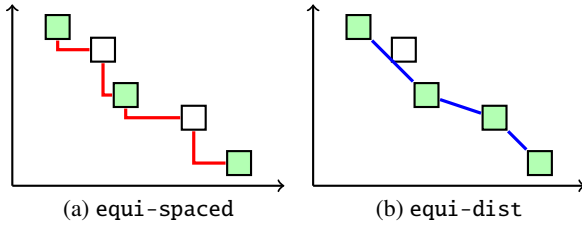


**Figure 2: Illustration of sampled solutions (green squares) by equi-spaced and equi-dist. equi-spaced uniformly samples solutions by walking along a Pareto front curve (red line) with roughly the same Manhattan distance. equi-dist uniformly samples solutions on a curve with roughly the same Euclidean distance.**

Figure 2 illustrates sampled solutions from equi-spaced and equi-dist. The main difference is whether the distance is measured on curve (Manhattan) or not (Euclidean).

We now describe a method called equi-jaccard that performs uniform sampling in non-objective space. We employ Jaccard distance to measure the dissimilarity between the coverage of two rule subsets. Formally, for two rule subsets  $\mathcal{R}_1$  and  $\mathcal{R}_2$ , their Jaccard distance is defined as  $\text{Jaccard}(\mathcal{R}_1, \mathcal{R}_2) = 1 - \frac{|\mathcal{D}(\mathcal{R}_1) \cap \mathcal{D}(\mathcal{R}_2)|}{|\mathcal{D}(\mathcal{R}_1) \cup \mathcal{D}(\mathcal{R}_2)|}$ .

Since this is a non-coordinate system, we think of all solutions on a Pareto front as a clique where edges between two solutions are weighed by their Jaccard distance. Now we can generate a traversal of all solutions on this graph to form a “curve” in this space, and then apply the same idea of equi-spaced so that Jaccard distance is roughly the same for two consecutive samples. There are many ways to perform a traversal. We can perform depth-first search on this graph to minimize or maximize the Jaccard distance of the overall path. We can also search for minimum sum of Jaccard distance of the traversal using the travelling salesperson (TSP) algorithm.<sup>3</sup> During our early investigation, we found that different methods lead to similar HV performance of the final Pareto front generated by PORS. Therefore, we only report results of equi-jaccard on a traversal generated by TSP algorithm.

**4.2.2 Non-uniform Sampling.** We consider the following methods of non-uniform sampling in the objective space.

- **hv-ss** [8]. hv-ss aims to select  $k$  solutions so that their hypervolume is maximized.
- **igd/igd+-ss** [8]. igd/igd+-ss aims to select  $k$  solutions so that their Inverted Generational Distance (IGD) or Inverted Generational Distance plus (IGD+) is minimized.
- **hvc-ss**. In this work, we propose to select  $k$  solutions so that their hypervolume contribution to the Pareto front in the last iteration is maximized. This is achieved using a greedy forward stepwise method to select  $k$  solutions.
- **k-medoids-pr** [7] (or **k-med.-pr** for short). This is the standard  $k$ -medoids clustering performed in the objective space (of precision and recall), with distance measured by Euclidean distance.

<sup>3</sup>TSP generates a loop with minimized overall distance. We cut the edge with the largest Jaccard distance on the loop to form a traversal path.

---

### Algorithm 2 Sequential Covering

---

```

1: procedure SEQUENTIALCOVERING( $\mathcal{D}, n, len, \beta$ )
2:    $\mathcal{R} \leftarrow \emptyset$ 
3:    $\mathcal{D}' \leftarrow \mathcal{D}$ 
4:   for  $i = 1$  to  $n$  do
5:      $r \leftarrow \text{RULEINDUCTION}(len, \beta, \mathcal{D}')$ 
6:      $\mathcal{D}' \leftarrow \mathcal{D}' \setminus \{x \mid r \text{ covers } x, x \in \mathcal{D}'\}$ 
7:      $\mathcal{R} \leftarrow \mathcal{R} \cup \{r\}$ 
   return  $\mathcal{R}$ 

```

---



---

### Algorithm 3 SpectralRules

---

```

1: procedure SPECTRALRULES( $\mathcal{D}, n, len, \mathcal{B}$ )
2:    $\mathcal{R} \leftarrow \emptyset$ 
3:   for  $\beta \in \mathcal{B}$  do
4:      $\mathcal{R} \leftarrow \mathcal{R} \cup \text{SEQUENTIALCOVERING}(\mathcal{D}, \lfloor \frac{n}{|\mathcal{B}|} \rfloor, len, \beta)$ 
   return  $\mathcal{R}$ 

```

---

We also consider  $k$ -medoids clustering performed on Jaccard distance measure, and introduce a non-uniform sampling in non-objective space method called **k-medoids-jaccard** (or **k-med.-j.** for short).

Since all those SSF methods have very efficient implementation, the complexity of each iteration of PORS is dominated by  $O(k|\mathcal{R}|+c)$ , where  $\mathcal{R}$  is the set of initial rules and  $c$  denotes the complexity of computing Pareto front (for Line 13 in Algorithm 1, and its worst case complexity is usually quadratic). Note that the time complexity mainly depends on the number of input rules, and depends less on dataset size. As we will see in Section 5.3.2, empirically we found all SSF methods are very efficient for different values of  $k$ .

Some of the aforementioned methods are studied in previous research in the context of EMO on continuous problems [21], but there is little research of all those 9 methods (covering 4 categories of the SSF problem) for combinatorial problems of finding Pareto-optimal rule subsets considered in this paper. To this end, we provide a thorough evaluation of those 9 methods in Section 5.

## 4.3 SpectralRules

The quality of initial rule set from Stage 1 may also impact the performance of Pareto-optimal rule subset selection. Existing approaches employ variants of tree ensemble to extract the initial rule set [16], which may generate a lot of “homogeneous” rules that look alike each other. Therefore, we introduce in this work a novel variant of sequential covering algorithm called SpectralRules to promote the diversity of the initial pool of rules for Stage 1.

We first review the sequential covering algorithm. Sequential covering is a “separate-and-conquer” procedure that repeatedly learns a single rule to create a rule set that covers the entire dataset rule by rule [13]. Algorithm 2 summarizes the classic sequential covering algorithm used in this work. We start with empty rule set  $\mathcal{R}$  and whole dataset  $\mathcal{D}$  (Line 2-3). We iteratively learn a rule  $r$  using standard rule induction that employs  $F_\beta$  as the evaluation metric to grow a rule up to a pre-specified length  $len$ , and then remove all points covered by  $r$  from the remaining dataset, until we find  $n$  rules (Line 4-7).

Dataset	Size	Attributes	Pos. Rate
Default	30,000	24	22.12%
Credit	150,000	11	6.68%
Fraud	284,807	31	0.17%
Bank	45,211	17	11.70%
A1	6,609,266	731	$\delta_1$
A2	990,798	210	$\delta_2$
A3	9,837,541	176	$\delta_3$

Table 2: Datasets.

A very small  $\beta$  (e.g., 0.1) can be employed to focus on mining high precision rules. However, recall of the rules produced by sequential covering might be quite limited in this case. As a result, we may end up with many rules of high precision and low recall, leading to a suboptimal rule set. To this end, we propose SpectralRules to encourage the diversity among rules. By diversity we mean rules of different level of precision and recall. This is achieved through multiple trials of Algorithm 2 with  $\beta$  ranging from small number (such as 0.01) to large number (such as 1).

Algorithm 3 summarizes the SpectralRules procedure. We are given a set  $\mathcal{B}$  with multiple  $\beta$ 's. For each  $\beta \in \mathcal{B}$ , we run Algorithm 2 with this specific  $\beta$  to generate at most  $\left\lceil \frac{n}{|\mathcal{B}|} \right\rceil$  rules (Line 3-4). The resulting rule set  $\mathcal{R}$  is composed of rules with different level of precision and recall. In this paper, we fix  $\mathcal{B} = \{0.01, 0.02, 0.04, 0.06, 0.08, 0.10, 0.20, 0.40, 0.60, 0.80\}$  and as we will see in our experiments, SpectralRules usually leads to Pareto fronts with higher HV (Section 5.2), and benefits Stage 2 accordingly with final rule subsets of higher quality (Section 5.4).

## 5 EXPERIMENTS

We report our results on both public datasets and proprietary datasets from Alipay. We release a repository of code that can fully reproduce the results (including tables and figures) in this section on public datasets [1].

### 5.1 Datasets

Table 2 summarizes the datasets used in our experiments. We use 4 public Fintech-related datasets in this paper. “Default” and “Bank” are from the UCI repository.<sup>4</sup> “Credit” is a binary classification problem that predicts the probability that somebody will experience financial distress in the next two years.<sup>5</sup> “Fraud” is a Kaggle competition problem that aims to recognize fraudulent credit card transactions.<sup>6</sup>

“A1”, “A2” and “A3” are three proprietary fraud prevention problems inside Alipay, representing three different fraudulent activities such as fraudulent payment transactions, identity theft, etc. Those datasets are large in scale and we do not reveal the positive ratio of each proprietary dataset by using  $\delta$  to symbolize the actual number.

### 5.2 Pareto-optimal Rule Subsets Evaluation

We first conduct a thorough evaluation of finding Pareto-optimal rule subsets. We consider classical EMO algorithm NSGA-II [11]

<sup>4</sup><http://archive.ics.uci.edu/ml/>

<sup>5</sup><https://www.kaggle.com/c/GiveMeSomeCredit/data>

<sup>6</sup><https://www.kaggle.com/mlg-ulb/creditcardfraud>

which is believed to perform well for bi-objective optimization problems [22].<sup>7</sup> Following standard practice [8], we equip NSGA-II with an unbounded external archive (UEA) to store all non-dominated solutions examined during the execution of the algorithm. We found that NSGA-II with UEA consistently achieves higher performance. We set the parameter *mutation\_rate* to 0.02 and *generations* to 1000 while using default values for other parameters. We observe this parameter setup often achieves the best results for NSGA-II. For our PORS framework, we consider all SSF methods listed in Section 4.2 to implement the framework. We use  $k = 10$  as the number of samples for SSF, which is the only parameter to set for SSF methods.

We consider two candidates for generating the initial rule set in Stage 1. We follow the same approach in [16] that uses a variant of tree ensemble (called TreeEns). We also employ SpectralRules proposed in this paper to generate the initial set of rules. For both methods, maximum rule length is fixed to 6 and we generate (up to) 500 rules from each method to form the initial rule set  $\mathcal{R}$ .

We use hypervolume indicator (HV) to measure the quality of Pareto-optimal rule subsets. For all experiments, we randomly partition the dataset into training (60% of the data), validation (20% of the data) and test sets (20% of the data). We generate the initial rule set in Stage 1 using training set. We then apply our 9 PORS algorithms and NSGA-II on the training set, select the best Pareto front with highest HV on the validation set and collect its HV on test set. All experiments are repeated 5 times and we report mean and standard deviation of the evaluation results on test sets.

Table 3 and 4 shows the HV results on test set for each dataset when the initial rule set is generated by TreeEns and SpectralRules, respectively. We first observe that PORS with *hvc-ss* as its SSF method consistently achieves the highest HV for both cases. In addition, we also observe that employing SpectralRules in Stage 1 leads to higher HV of the final Pareto front by comparing the best values in Table 3 and 4. Therefore, we recommend implementing PORS framework with *hvc-ss* as its SSF method, and with some abuse of notation, we now refer to this particular combination as the PORS algorithm.

**Intuitive explanation of why *hvc-ss* performs the best.** PORS framework can be viewed as a greedy forward stage-wise algorithm, with maximizing HV as its objective, by gradually expanding Pareto fronts. Among all SSF methods, *hvc-ss* achieves the largest HV increase (by definition) for each iteration (Pareto front expansion), and therefore it should work well inside PORS framework. Because of the greedy nature of the framework, other SSF methods might also work well. Our empirical study complements the picture and shows *hvc-ss* indeed achieves the best results on most cases.

### 5.3 Discussion

In this section, we provide more experimental results to shed light on properties of different combinations of methods.

**5.3.1 Comparison of SpectralRules and TreeEns.** It is apparent that the quality of the initial rule set  $\mathcal{R}$  from Stage 1 may have significant impact for the final Pareto front; it is impossible to find high-quality rule subsets when some key rules are not present in

<sup>7</sup>We use pyMultiobjective package at <https://github.com/Valdecy/pyMultiobjective>

Type	Method	Default	Credit	Fraud	Bank	A1	A2	A3	
EMO	NSGA-II [11]	0.524±0.013	0.322±0.023	0.786±0.027	0.533±0.018	0.296±0.010	0.169±0.006	0.032±0.006	
unif.	obj.	equi-spaced [18]	0.515±0.008	0.323±0.021	0.783±0.020	0.517±0.020	0.299±0.011	0.172±0.006	0.033±0.006
		equi-dist	0.517±0.010	0.324±0.022	0.786±0.021	0.528±0.014	0.298±0.010	0.173±0.006	0.034±0.006
	non-obj.	equi-jaccard	0.509±0.007	0.308±0.018	0.789±0.032	0.516±0.019	0.296±0.012	0.166±0.009	0.033±0.006
non-unif.	obj.	hv-ss [8]	0.519±0.009	0.325±0.022	0.783±0.037	0.530±0.021	0.298±0.007	0.165±0.007	0.034±0.005
		igd-ss [8]	0.496±0.012	0.297±0.023	0.790±0.038	0.499±0.021	0.297±0.012	0.163±0.006	0.031±0.007
		igd+-ss [8]	0.491±0.010	0.281±0.018	0.789±0.031	0.480±0.025	0.289±0.011	0.147±0.008	0.027±0.004
		hvc-ss	<b>0.524±0.011</b>	<b>0.325±0.022</b>	<b>0.798±0.040</b>	<b>0.533±0.015</b>	<b>0.301±0.012</b>	<b>0.176±0.006</b>	<b>0.036±0.006</b>
		k-medoids-pr [7]	0.501±0.013	0.303±0.025	0.785±0.027	0.511±0.020	0.296±0.014	0.170±0.005	0.031±0.007
	non-obj.	k-medoids-jaccard	0.472±0.016	0.258±0.035	0.792±0.034	0.479±0.026	0.284±0.012	0.142±0.006	0.024±0.010

**Table 3: The hypervolume (HV) performance (mean±std) of the Pareto front for different methods on test set of each problem. Higher HV is better and best method for each dataset is marked in bold. TreeEns [16] is employed in Stage 1 to produce the initial 500 rules.**

Type	Method	Default	Credit	Fraud	Bank	A1	A2	A3	
EMO	NSGA-II [11]	0.526±0.013	0.350±0.011	0.789±0.036	0.585±0.011	0.313±0.004	0.188±0.005	0.033±0.004	
unif.	obj.	equi-spaced [18]	0.534±0.012	0.350±0.014	0.796±0.037	0.570±0.009	0.313±0.006	0.183±0.007	0.035±0.006
		equi-dist	0.535±0.011	0.352±0.015	0.805±0.025	0.575±0.009	0.315±0.005	0.180±0.008	0.034±0.006
	non-obj.	equi-jaccard	0.535±0.014	0.357±0.014	0.803±0.028	0.577±0.013	0.314±0.009	0.176±0.008	0.034±0.007
non-unif.	obj.	hv-ss [8]	0.534±0.011	0.357±0.016	0.801±0.033	0.582±0.008	0.318±0.004	0.184±0.006	0.035±0.005
		igd-ss [8]	0.516±0.015	0.346±0.016	0.798±0.045	0.560±0.012	0.317±0.006	0.185±0.006	0.033±0.007
		igd+-ss [8]	0.515±0.016	0.338±0.012	0.793±0.024	0.553±0.017	0.308±0.005	0.160±0.007	0.029±0.004
		hvc-ss	<b>0.540±0.012</b>	<b>0.359±0.013</b>	<b>0.808±0.030</b>	<b>0.593±0.012</b>	<b>0.319±0.006</b>	<b>0.192±0.007</b>	<b>0.036±0.005</b>
		k-medoids-pr [7]	0.515±0.013	0.343±0.014	0.801±0.033	0.563±0.009	0.317±0.004	0.184±0.005	0.033±0.006
	non-obj.	k-medoids-jaccard	0.507±0.016	0.333±0.011	0.791±0.030	0.521±0.014	0.301±0.011	0.151±0.006	0.028±0.008

**Table 4: The hypervolume (HV) performance (mean±std) of the Pareto front for different methods on test set of each problem. Higher HV is better and best method for each dataset is marked in bold. SpectralRules is employed in Stage 1 to produce the initial 500 rules.**

Dataset	k	hvc-ss	hv-ss	igd-ss	igd+-ss	k-med.-pr	k-med.-j.	equi-j.	equi-spaced	equi-dist
Bank	5	0.575±0.009	<b>0.583±0.011</b>	0.531±0.014	0.502±0.025	0.549±0.012	0.493±0.022	0.552±0.012	0.555±0.009	0.561±0.01
	10	<b>0.591±0.012</b>	0.580±0.009	0.546±0.017	0.539±0.016	0.562±0.010	0.512±0.013	0.564±0.015	0.571±0.009	0.571±0.010
	15	<b>0.596±0.011</b>	0.582±0.010	0.564±0.013	0.553±0.014	0.566±0.008	0.533±0.018	0.567±0.012	0.574±0.006	0.577±0.008
	20	<b>0.594±0.011</b>	0.583±0.010	0.561±0.011	0.554±0.013	0.571±0.011	0.531±0.011	0.568±0.014	0.574±0.006	0.578±0.008
Credit	5	0.347±0.012	<b>0.350±0.011</b>	0.333±0.010	0.325±0.012	0.337±0.010	0.316±0.008	0.342±0.016	0.340±0.016	0.341±0.012
	10	<b>0.357±0.012</b>	0.356±0.015	0.345±0.014	0.336±0.011	0.345±0.011	0.331±0.011	0.355±0.013	0.350±0.013	0.351±0.015
	15	<b>0.359±0.015</b>	0.358±0.014	0.348±0.014	0.340±0.012	0.349±0.013	0.337±0.011	0.356±0.013	0.353±0.013	0.356±0.014
	20	<b>0.359±0.015</b>	0.358±0.014	0.352±0.014	0.342±0.011	0.350±0.014	0.341±0.012	0.356±0.013	0.355±0.013	0.357±0.013
Default	5	<b>0.541±0.014</b>	0.532±0.013	0.501±0.021	0.509±0.022	0.512±0.014	0.495±0.019	0.532±0.010	0.529±0.012	0.534±0.012
	10	<b>0.540±0.012</b>	0.535±0.010	0.517±0.015	0.515±0.016	0.515±0.013	0.504±0.021	0.535±0.009	0.534±0.012	0.535±0.011
	15	<b>0.536±0.012</b>	0.535±0.011	0.524±0.016	0.525±0.018	0.523±0.015	0.510±0.015	0.535±0.010	0.536±0.011	0.536±0.010
	20	0.533±0.011	<b>0.537±0.010</b>	0.525±0.012	0.525±0.013	0.527±0.014	0.514±0.015	0.534±0.012	0.536±0.011	<b>0.537±0.010</b>
Fraud	5	<b>0.805±0.031</b>	0.794±0.034	0.801±0.026	0.798±0.024	0.802±0.030	0.786±0.035	0.794±0.027	0.793±0.039	0.790±0.034
	10	<b>0.808±0.030</b>	0.801±0.033	0.798±0.045	0.794±0.026	0.793±0.032	0.800±0.029	0.803±0.028	0.796±0.037	0.805±0.025
	15	0.806±0.032	0.801±0.032	<b>0.809±0.030</b>	0.806±0.032	0.802±0.035	0.804±0.029	0.808±0.025	0.797±0.036	0.807±0.028
	20	0.801±0.037	0.797±0.045	0.797±0.048	0.807±0.026	<b>0.808±0.033</b>	0.797±0.035	0.793±0.047	0.806±0.033	0.804±0.040

**Table 5: The hypervolume (HV) performance (mean±std) of the Pareto front for different methods on test set of each problem. Higher HV is better. SpectralRules is employed in Stage 1 to produce the initial 500 rules. The maximum round running of PORS is set to 30 to avoid early stopping, i.e., each experiment trial fully completed 30 iterations.**

$\mathcal{R}$  in the first place. Section 5.2 demonstrates that SpectralRules outperforms TreeEns when the size of  $\mathcal{R}$  is set to 500. In this section, we provide further investigation on the effects of SpectralRules and TreeEns when the size of  $\mathcal{R}$  varies. In this experiment, we use PORS algorithm as our method to find Pareto-optimal rule subsets.

Figure 3 illustrates the HV performance on Bank dataset when the size of  $\mathcal{R}$  increases. Results are aggregated over 5 trials of random partitioning of the dataset. We observe that SpectralRules outperforms TreeEns for all  $|\mathcal{R}| \leq 500$ . SpectralRules cannot produce a larger rule set since all positive points are already covered with

Dataset	k	hvc-ss	hv-ss	igd-ss	igd+-ss	k-med.-pr	k-med.-j.	equi-j.	equi-spaced	equi-dist
Bank	5	47.36±2.00	47.36±2.00	46.71±0.80	47.09±2.13	44.85±0.94	59.33±3.25	48.10±4.76	44.02±1.68	44.65±1.73
	10	64.27±4.08	53.61±3.08	57.44±2.16	58.02±2.95	53.62±3.05	73.65±2.70	65.63±2.55	52.64±2.19	52.21±2.59
	15	83.45±4.23	57.56±1.82	69.57±4.38	66.63±3.65	60.31±3.89	93.31±3.93	73.08±1.16	55.72±1.29	56.26±2.15
	20	113.47±4.22	62.71±1.11	80.73±4.80	75.91±1.23	62.19±2.07	110.80±4.50	81.95±4.08	62.28±2.74	61.53±2.47
Credit	5	57.45±6.17	48.92±5.83	58.95±6.63	49.92±2.17	48.03±3.61	125.73±15.02	68.48±5.81	45.31±1.19	48.92±3.68
	10	93.31±9.57	63.53±4.56	90.76±6.50	73.82±4.17	61.64±4.28	238.02±25.20	121.91±12.10	57.66±3.41	61.02±8.11
	15	140.18±10.64	70.92±4.03	121.71±12.48	93.68±2.77	68.72±4.27	350.31±22.91	161.11±8.78	66.79±2.86	71.79±11.58
Default	5	49.19±2.19	43.57±2.35	49.69±2.29	47.44±1.78	41.26±1.07	53.80±3.85	57.73±2.32	41.82±1.03	43.08±1.74
	10	71.33±4.34	54.12±5.40	66.04±4.95	63.25±3.70	49.20±3.36	71.20±2.21	79.19±3.06	51.53±2.41	49.99±1.75
	15	99.13±3.36	60.22±4.73	80.24±1.89	79.72±6.15	54.43±2.38	93.06±6.31	96.18±4.66	56.71±2.01	55.31±1.72
	20	133.09±10.86	67.49±5.00	101.47±2.29	98.13±3.53	61.73±3.17	116.56±4.28	113.25±5.85	61.16±1.81	61.50±1.45
Fraud	5	40.42±0.16	40.81±1.03	41.35±1.05	42.23±0.81	41.15±0.55	61.24±1.63	42.40±0.52	42.23±0.54	42.20±0.55
	10	45.75±1.00	45.62±1.14	46.94±0.74	47.88±1.52	46.68±0.81	74.92±1.87	48.86±1.23	47.35±1.36	47.44±1.85
	15	50.88±0.84	50.06±0.43	51.90±1.41	52.43±0.80	50.34±0.52	87.41±2.18	51.62±1.31	50.27±0.31	50.49±0.91
	20	56.71±2.46	53.91±0.63	55.59±1.22	56.99±0.99	54.65±0.68	100.30±1.85	55.06±1.58	54.12±0.58	53.56±0.41

**Table 6: The running time (mean±std) for different methods on test set of each problem. SpectralRules is employed in Stage 1 to produce the initial 500 rules. The maximum round running of PORS is set to 30 to avoid early stopping, i.e., each experiment trial fully completed 30 iterations.**

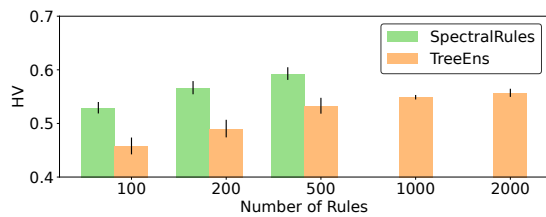


**Figure 3: HV of PORS algorithm on Bank dataset when using SpectralRules or TreeEns to produce rule set in Stage 1.**

500 rules. We also observe that even if we give more budget on the number of rules to TreeEns, it cannot catch up with the level of HV achieved by SpectralRules. Similar patterns are observed on other datasets.

There exist some key differences between SpectralRules and TreeEns. TreeEns extracts rules from a tree ensemble, and therefore we expect that there are many “homogeneous” rules (in terms of the distribution of precision and recall for all rules in the set) that look alike each other. This not only hurts the efficiency of the subsequent subset selection but the efficacy of that also takes a hit. On the other hand, SpectralRules employs direct rule induction and focuses on promoting the diversity of  $\mathcal{R}$ , leading to a more compact rule set of higher quality. On Bank dataset, for  $|\mathcal{R}| = 500$ , we observe the mean and standard deviation for precision (recall) of TreeEns and SpectralRules is  $0.5461 \pm 0.1604$  ( $0.0225 \pm 0.0330$ ) and  $0.6376 \pm 0.1823$  ( $0.0381 \pm 0.0699$ ), respectively. We see that not only the mean of precision (recall) from SpectralRules is higher, its standard deviation is larger as well. Hence, for the rest of this paper, we use SpectralRules for Stage 1 by default unless otherwise mentioned.

**5.3.2 Impact of Different Values of  $k$ .** To further evaluate the impact of different values of  $k$  on PORS with different SSF methods, including running time and HV, we set  $k$  to 5, 10, 15, 20 respectively

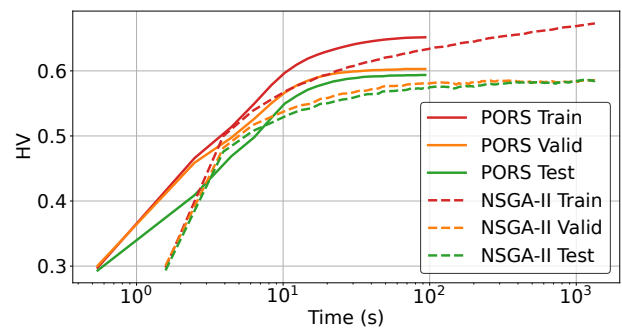


**Figure 4: Efficiency of NSGA-II vs. PORS on Bank dataset.**

and apply those 9 PORS algorithms on the 4 public datasets. According to previous sections, SpectralRules is employed in Stage 1 and the maximum round running of PORS is set to 30 to avoid early stopping, i.e., each experiment trial fully completed 30 iterations. All experiments are repeated 5 times.

Table 5 shows the HV results on test set of different PORS algorithms for each  $k$ . Once again, we observe that PORS with hvc-ss as its SSF method achieves the highest HV on most cases. For all SSF methods, a larger value of  $k$  usually leads to a higher HV as expected. However, once the  $k$  exceeds 10, the increase in HV usually becomes so tiny to be significant.

The running time of PORS is positively correlated to the value of  $k$  as shown in Table 6. Considering the trade-off between performance and efficiency, we recommend to use  $k = 10$  in practice.

**5.3.3 Efficiency Evaluation for EMO and PORS Algorithm.** From Section 5.2 we observe that NSGA-II as an EMO algorithm is a very competitive to PORS algorithm. In this section, we conduct efficiency evaluation for these two methods. We run both algorithms on a standard server with 16GB memory using 4 threads.



Dataset	Prec	CRSL [16]	PORS		
			hvc-ss (High HV)	equi-spaced (Med. HV)	k-med.-j. (Low HV)
Default	0.3	0.765±0.025	<b>0.854±0.010</b>	0.853±0.013	0.835±0.014
	0.5	0.519±0.012	0.557±0.020	<b>0.564±0.005</b>	0.543±0.017
	0.7	0.238±0.038	0.260±0.040	<b>0.262±0.052</b>	0.257±0.045
Credit	0.3	0.555±0.030	<b>0.584±0.013</b>	0.581±0.015	0.538±0.012
	0.5	0.269±0.059	<b>0.289±0.017</b>	0.279±0.037	0.273±0.030
	0.7	0.038±0.021	<b>0.041±0.013</b>	0.025±0.023	0.024±0.023
Fraud	0.3	0.840±0.038	<b>0.851±0.045</b>	0.847±0.035	0.836±0.037
	0.5	0.816±0.024	0.822±0.035	0.822±0.038	<b>0.822±0.024</b>
	0.7	0.812±0.032	0.814±0.021	<b>0.818±0.033</b>	0.808±0.034
Bank	0.3	0.907±0.015	<b>0.951±0.007</b>	0.945±0.009	0.813±0.034
	0.5	0.630±0.075	<b>0.781±0.018</b>	0.764±0.034	0.679±0.050
	0.7	<b>0.337±0.044</b>	0.264±0.044	0.243±0.038	0.253±0.055
A1	5 $\delta_1$	0.789±0.023	<b>0.824±0.013</b>	0.794±0.016	0.775±0.021
	10 $\delta_1$	0.624±0.016	<b>0.657±0.011</b>	0.640±0.012	0.614±0.018
	20 $\delta_1$	0.499±0.008	<b>0.510±0.009</b>	0.501±0.006	0.487±0.009
A2	5 $\delta_2$	0.828±0.019	<b>0.831±0.007</b>	0.767±0.012	0.726±0.009
	10 $\delta_2$	0.483±0.072	<b>0.593±0.008</b>	0.578±0.008	0.545±0.009
	20 $\delta_2$	0.263±0.079	0.324±0.017	<b>0.326±0.006</b>	0.292±0.006
A3	5 $\delta_3$	<b>0.581±0.022</b>	0.563±0.019	0.543±0.054	0.483±0.034
	10 $\delta_3$	0.531±0.028	<b>0.560±0.021</b>	0.526±0.037	0.453±0.034
	20 $\delta_3$	0.387±0.033	<b>0.414±0.011</b>	0.402±0.023	0.381±0.021

**Table 7: CRSL vs PORS.** Each cell represents the recall on test set (mean± std) under a corresponding precision threshold. For propriety datasets, we use the precision threshold of 5x, 10x, 20x of the positive rate of the dataset. The best method is marked in bold for each case.

Figure 4 shows how HV changes on train, valid and test sets of Bank dataset over wall clock time for NSGA-II and PORS algorithm. We can see that PORS algorithm quickly converges while NSGA-II is less efficient. Similar patterns are observed on other datasets.

In particular, on our largest dataset A3, PORS takes 146 seconds to finish while NSGA-II takes 1610 seconds on the same server with 16GB using 4 threads. This suggests a heuristic-based algorithm can be highly efficient.

## 5.4 Case Study

In this section, we provide two case studies within Alipay where the requirement of the final rule subset of Stage 2 differs, and demonstrate how finding Pareto-optimal rule sets as an intermediate stage between Stage 1 and Stage 2 can benefit the eventual result.

To study the relationship of HV (as an intermediate evaluation metric) and final objective, we consider three implementations of PORS framework in this section; hvc-ss for high HV, equi-spaced for medium HV, and k-med.-j. for low HV.

**5.4.1 Confidence-Constrained Rule Set Learning.** We consider confidence-constrained rule set learning (CRSL) [16] as our first case study. This learning paradigm seeks to maximize recall constrained on some precision threshold, and there are many similar application scenarios inside Alipay that fall in this paradigm. Note that CRSL only works on TreeEnns as it needs a large candidate set to select from, and we compare it with PORS algorithms using SpectralRules for Stage 1.

Table 7 summarizes results on both public and propriety datasets for CRSL and PORS algorithms. We observe that on both public and propriety datasets, PORS with hvc-ss outperforms CRSL on most cases. In addition, we observe that there is a positive correlation

Dataset	$\beta$	Greedy	PORS		
			hvc-ss (High HV)	equi-spaced (Med. HV)	k-med.-j. (Low HV)
Default	0.1	0.743±0.039	<b>0.762±0.033</b>	0.747±0.022	0.732±0.007
	0.2	0.685±0.015	0.687±0.015	<b>0.692±0.019</b>	0.685±0.012
	0.5	0.573±0.014	0.578±0.008	0.577±0.011	<b>0.582±0.014</b>
Credit	0.1	0.608±0.043	<b>0.616±0.035</b>	0.608±0.039	0.611±0.034
	0.2	0.523±0.020	0.536±0.015	<b>0.540±0.025</b>	0.534±0.025
	0.5	0.431±0.011	0.433±0.009	<b>0.434±0.007</b>	0.426±0.011
Fraud	0.1	<b>0.973±0.006</b>	0.968±0.013	0.959±0.023	0.957±0.011
	0.2	0.935±0.029	<b>0.950±0.007</b>	0.941±0.016	0.946±0.008
	0.5	0.838±0.032	<b>0.888±0.021</b>	0.887±0.021	0.873±0.019
Bank	0.1	0.755±0.017	<b>0.763±0.020</b>	0.709±0.016	0.729±0.016
	0.2	0.652±0.017	<b>0.682±0.015</b>	0.666±0.018	0.656±0.017
	0.5	0.596±0.009	<b>0.603±0.010</b>	0.596±0.012	0.586±0.010
A1	0.1	0.689±0.011	<b>0.695±0.009</b>	0.682±0.009	0.674±0.010
	0.2	0.592±0.010	<b>0.599±0.006</b>	0.599±0.009	0.590±0.010
	0.5	0.446±0.004	<b>0.451±0.006</b>	0.443±0.003	0.439±0.007
A2	0.1	0.543±0.045	<b>0.547±0.039</b>	0.543±0.044	0.535±0.020
	0.2	0.443±0.018	<b>0.446±0.025</b>	0.438±0.024	0.429±0.017
	0.5	0.290±0.012	0.290±0.012	<b>0.304±0.011</b>	0.289±0.009
A3	0.1	<b>0.257±0.183</b>	0.250±0.114	0.240±0.119	0.222±0.139
	0.2	0.119±0.076	<b>0.127±0.062</b>	0.126±0.060	0.119±0.068
	0.5	0.067±0.029	<b>0.074±0.019</b>	0.065±0.017	0.063±0.009

**Table 8: Greedy vs PORS.** Each cell represents the  $F_\beta$  score on test set (mean± std) under a particular  $\beta$ . The best method is marked in bold for each case.

between HV (as an intermediate evaluation metric) and recall (as a final objective).

Note that CRSL needs to run on each precision threshold to produce a rule subset, while PORS algorithm only needs to run once and it generates a set of rule subsets that can be readily picked up for different precision thresholds. Such flexibility is usually appreciated in real development of rule subsets as rule mining in practice is typically an explorative and iterative process.

**5.4.2 Rule Set Learning Using  $F_\beta$  Score.** As our second case study, we use  $F_\beta$  score to select the final rule subsets for Stage 2 (which is also widely used inside Alipay). Note that for Fintech applications, a small  $\beta$  is usually favored so that the metric is more biased towards precision. We compare PORS with standard greedy forward stepwise algorithm for subset selection (Greedy), both using SpectralRules to produce a initial rule set of 500 rules in Stage 1. The greedy algorithm iteratively adds one rule from the initial rule set so as to achieve the highest metric value. To avoid running into local optima, we equip Greedy with beam search of width 10.

Table 8 summarizes results on both public and propriety datasets for Greedy and PORS algorithms. We can see that PORS with hvc-ss outperforms Greedy by finding rule subsets with higher  $F_\beta$  on most cases. We again observe that the positive correlation between HV (as an intermediate evaluation metric) and  $F_\beta$  (as a final objective). Note that Greedy needs to run multiple times (one for each  $\beta$ ) while PORS only needs to run once and it generates a set of Pareto-optimal rule subsets. It gives more flexibility for human to quickly experiment different  $\beta$ s without additional effort.

We note that both Greedy and PORS adds one rule for each iteration, and therefore we can compare the running time in a relatively fair fashion. Hence, we run both Greedy and PORS (with hvc-ss) algorithm on a standard server with 16GB memory using 4 threads. Figure 5 illustrates the running time for PORS and Greedy

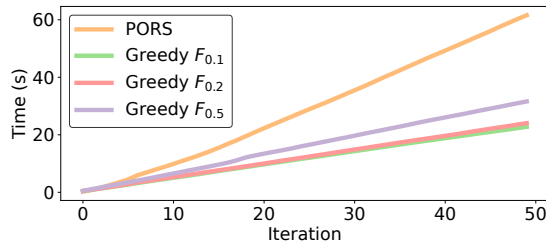


Figure 5: Running time for Greedy and PORS on Bank dataset.

$F_{0.1}$ ,  $F_{0.2}$ , and  $F_{0.5}$  on Bank dataset. As expected,  $\beta$  has little impact on the running time for Greedy. Since PORS aims to generate a set of rule subsets while Greedy only focuses on one single metric, PORS needs to do more work for each iteration and we empirically observe PORS takes 2x to 3x more time than single run of Greedy for each iteration. This is acceptable in practice given the flexibility offered by PORS.

## 5.5 Online Evaluation

We perform an online A/B testing for PORS algorithm (with `hvc-ss`) and CRSL [16] from 12/06/2023 to 12/27/2023. These two algorithms are trained on a same anti-money laundering dataset with 5,532,623 points and 717 features. The precision threshold has been set to 0.8 and the goal is to maximize recall. These two algorithms both produce rule subsets of 22 rules.

In accordance with Alipay's non-disclosure policy, we report the relative increase of recall rather than the actual number in this paper. PORS achieved 1.56% increase of recall while CRSL achieved 1.49% increase of recall; significant with  $p$ -value = 0 from two-tailed paired  $t$ -test on 59 million samples.

We have deployed our PORS algorithm in our internal Fanglue system [19] and it has been serving our anti-money laundering team for more than 6 months.

## 6 CONCLUSION

In practice, a two-stage framework of fraud prevention decision rule set mining is usually employed in large Fintech institutions. This paper aims to find high-quality rule subsets in a bi-objective space of precision and recall when some initial pool of rules are given. To this end, we adopt the concept of Pareto optimality and aim to find a set of non-dominated rule subsets, which constitutes a Pareto front. We propose a heuristic-based framework called PORS and we identify that the core of PORS is the problem of solution selection on the front (SSF). We provide a systematic categorization of the SSF problem and a thorough empirical evaluation of various SSF methods. We also propose a novel variant of sequential covering algorithm called SpectralRules to encourage the diversity of the initial rule set and

we empirically find that SpectralRules further improves the quality of the found Pareto front. On two real application scenarios within Alipay, we demonstrate the advantages of our proposed methodology compared to existing work.

## REFERENCES

- [1] 2024. *GitHub repo*. <https://github.com/ChengyaoWen/Pareto-Optimal-Rule-Subset-Selection>
- [2] R. Agrawal, T. Imieliński, and A. Swami. 1993. Mining association rules between sets of items in large databases. In *SIGMOD*.
- [3] J. Bader and E. Zitzler. 2011. HypE: An algorithm for fast hypervolume-based many-objective optimization. *Evolutionary computation* 19, 1 (2011), 45–76.
- [4] N. Beume, B. Naujoks, and M. Emmerich. 2007. SMS-EMOA: Multiobjective selection based on dominated hypervolume. *European Journal of Operational Research* 181, 3 (2007), 1653–1669.
- [5] L. Breiman. 2001. Random forests. *Machine learning* 45, 1 (2001), 5–32.
- [6] L. Breiman, J.H. Friedman, C.J. Stone, and R.A. Olshen. 1984. *Classification and regression trees*. Chapman and Hall/CRC.
- [7] W. Chen, H. Ishibuchi, and K. Shang. 2021. Clustering-based subset selection in evolutionary multiobjective optimization. In *SMC*.
- [8] W. Chen, H. Ishibuchi, and K. Shang. 2021. Fast Greedy Subset Selection From Large Candidate Solution Sets in Evolutionary Multiobjective Optimization. *IEEE Transactions on Evolutionary Computation* 26, 4 (2021), 750–764.
- [9] P. Clark and T. Niblett. 1989. The CN2 induction algorithm. *Machine learning* 3, 4 (1989), 261–283.
- [10] W.W. Cohen. 1995. Fast effective rule induction. In *ICML*.
- [11] K. Deb, A. Pratap, S. Agarwal, and T. Meyarivan. 2002. A fast and elitist multiobjective genetic algorithm: NSGA-II. *IEEE Transactions on Evolutionary Computation* 6, 2 (2002), 182–197.
- [12] A.P. Guerreiro, C.M. Fonseca, and L. Paquete. 2020. The Hypervolume Indicator: Problems and Algorithms. *arXiv preprint arXiv:2005.00515* (2020).
- [13] H. Lakkaraju, S.H. Bach, and J. Leskovec. 2016. Interpretable decision sets: A joint framework for description and prediction. In *KDD*.
- [14] B. Li, J. Li, K. Tang, and X. Yao. 2015. Many-objective evolutionary algorithms: A survey. *ACM Computing Surveys (CSUR)* 48, 1 (2015), 1–35.
- [15] M. Li and X. Yao. 2019. Quality evaluation of solution sets in multiobjective optimisation: A survey. *Comput. Surveys* 52, 2 (2019), 1–38.
- [16] M. Li, L. Yu, Y.-L. Zhang, X. Huang, Q. Shi, Q. Cui, X. Yang, L. Li, W. Zhu, Y. Fang, and J. Zhou. 2022. An Adaptive Framework for Confidence-constraint Rule Set Learning Algorithm in Large Dataset. In *CIKM*.
- [17] C. Molnar. 2020. *Interpretable Machine Learning*. Lulu. com.
- [18] V. Pereyra, M. Saunders, and J. Castillo. 2013. Equispaced Pareto front construction for constrained bi-objective optimization. *Mathematical and Computer Modelling* 57, 9-10 (2013), 2122–2131.
- [19] C. Qian, S. Liang, Z. Wang, and Y. Lou. 2023. Fanglue: An Interactive System for Decision Rule Crafting. *Proceedings of the VLDB Endowment* 16, 12 (2023), 4062–4065.
- [20] J.R. Quinlan. 1993. *C4. 5: programs for machine learning*. Morgan Kaufmann Publishers.
- [21] K. Shang, T. Shu, H. Ishibuchi, Y. Nan, and L.M. Pang. 2022. Benchmarking subset selection from large candidate solution sets in evolutionary multi-objective optimization. *arXiv preprint arXiv:2201.06700* (2022).
- [22] R. Tanabe, H. Ishibuchi, and A. Oyama. 2017. Benchmarking multi-and many-objective evolutionary algorithms under two optimization scenarios. *IEEE Access* 5 (2017), 19597–19619.
- [23] C.J. Van Rijsbergen. 1979. *Information Retrieval*. Butterworth-Heinemann.
- [24] G. Zhang and A. Gionis. 2020. Diverse Rule Sets. In *KDD*.
- [25] Q. Zhang and H. Li. 2007. MOEA/D: A multiobjective evolutionary algorithm based on decomposition. *IEEE Transactions on evolutionary computation* 11, 6 (2007), 712–731.
- [26] E. Zitzler. 1999. *Evolutionary algorithms for multiobjective optimization: Methods and applications*. Ph. D. Dissertation. ETH Zurich, Switzerland.
- [27] E. Zitzler, M. Laumanns, and L. Thiele. 2001. *SPEA2: Improving the strength Pareto evolutionary algorithm*. Technical Report. ETHZ, Zürich, Switzerland.